PROCEEDINGS B

rspb.royalsocietypublishing.org

Research

Cite this article: Lelièvre Y, Legendre P, Matabos M, Mihály S, Lee RW, Sarradin P-M, Arango CP, Sarrazin J. 2017 Astronomical and atmospheric impacts on deep-sea hydrothermal vent invertebrates. *Proc. R. Soc. B* **284**: 20162123.
http://dx.doi.org/10.1098/rspb.2016.2123

Received: 15 December 2016
Accepted: 8 March 2017

Subject Category:
Ecology

Subject Areas:
ecology

Keywords:
deep-sea observatory, hydrothermal vents, macrofaunal abundance, surface storms, ocean tides, time-series analysis

Author for correspondence:
Yann Lelièvre
e-mail: yann.lelievre@ifremer.fr

Electronic supplementary material is available online at https://dx.doi.org/10.6084/m9.figshare.c.3723970.

THE ROYAL SOCIETY PUBLISHING

Astronomical and atmospheric impacts on deep-sea hydrothermal vent invertebrates

Yann Lelièvre[1,2], Pierre Legendre[2], Marjolaine Matabos[1], Steve Mihály[3], Raymond W. Lee[4], Pierre-Marie Sarradin[1], Claudia P. Arango[5] and Jozée Sarrazin[1]

[1]Ifremer Centre de Bretagne, REM/EEP, Laboratoire Environnement Profond, 29280 Plouzané, France
[2]Département de sciences biologiques, Université de Montréal, C.P. 6128, succursale Centre-ville, Montréal, Québec, Canada H3C 3J7
[3]Ocean Networks Canada, University of Victoria, PO Box 1700 STN CSC, Victoria, British Columbia, Canada V8 W 2Y2
[4]School of Biological Sciences, Washington State University, Pullman, WA 99164, USA
[5]Biodiversity Program, Queensland Museum, PO BOX 3300, South Brisbane, Queensland 4101, Australia

YL, 0000-0003-3508-418X

Ocean tides and winter surface storms are among the main factors driving the dynamics and spatial structure of marine coastal species, but the understanding of their impact on deep-sea and hydrothermal vent communities is still limited. Multidisciplinary deep-sea observatories offer an essential tool to study behavioural rhythms and interactions between hydrothermal community dynamics and environmental fluctuations. Here, we investigated whether species associated with a *Ridgeia piscesae* tubeworm vent assemblage respond to local ocean dynamics. By tracking variations in vent macrofaunal abundance at different temporal scales, we provide the first evidence that tides and winter surface storms influence the distribution patterns of mobile and non-symbiotic hydrothermal species (i.e. pycnogonids *Sericosura* sp. and Polynoidae polychaetes) at more than 2 km depth. Local ocean dynamics affected the mixing between hydrothermal fluid inputs and surrounding seawater, modifying the environmental conditions in vent habitats. We suggest that hydrothermal species respond to these habitat modifications by adjusting their behaviour to ensure optimal living conditions. This behaviour may reflect a specific adaptation of vent species to their highly variable habitat.

1. Introduction

Benthic communities associated with hydrothermal vents have been extensively studied since their discovery in 1977 on the Galápagos Ridge [1]. Vent communities, relying on local chemosynthetic microbial production, are characterized by low diversity, large biomass and high levels of endemic species [2]. Within a single vent site, the high spatial and temporal variability of vent emissions creates a mosaic of habitats with contrasting physical and chemical conditions [3]. The resulting spatial distribution of species reflects the interplay between their physiological tolerance to environmental conditions [4,5], resource availability [6,7] and biotic factors [8,9]. The temporal and spatial variability of this unstable environment plays a key role in the functioning of these ecosystems.

The hydrothermal ecosystems of the World's oceans are subject to a variety of forces that create variability along a spatial (from centimetre to hundreds of kilometres) and temporal (from seconds to years) continuum. At broad spatial and temporal scales, the stability of hydrothermal activity and site lifespan are linked to geodynamic processes, such as tectonic or volcanic events, that can cause important physical, chemical and biological changes [10,11]. On small spatial scales (metres), mixing of hot hydrothermal fluids (up to 400°C) with cold ambient seawater (less than 2°C) creates steep spatial gradients of environmental variables [12,13]. On short timescales, temporal fluctuations of

© 2017 The Author(s) Published by the Royal Society. All rights reserved.

temperature and chemical conditions result from the variability of turbulent mixing of hydrothermal fluids with the ambient seawater, which is controlled both by the variability in fluid flux and of local oceanic currents. These deep-sea currents can be forced astronomically through the periodic variability of surface tides [14–16] and atmospherically by the passage of storms [16,17].

Although ocean tides are one of the most important factors controlling intertidal communities [18], their action on deep-sea communities is less understood. Nevertheless, the influence of tidal forcing on vent abiotic habitat conditions has been reported from various localities in the Atlantic [19,20] and Pacific Oceans [14,15,21]. Tide-related variability in hydrothermal biotopes is attributed to two mechanisms, including oceanic tidal pressure and modulation of horizontal bottom currents by ocean tides [14,20]. Ocean tides may affect faunal distributions by periodically altering the mixing of seawater with vent fluids. Mixing variability may directly influence the ambient temperature [14,15], the chemical environment [22], the bioavailability of potentially toxic compounds [23] and the exposure to radionuclides [24]. However, few studies have managed to verify this hypothesis in the absence of high-resolution temporal data. To our knowledge, tidal influence has only been detected in two symbiotic vent taxa: (*i*) *Bathymodiolus* spp. growth rates [25–27] and (*ii*) *Ridgeia piscesae* branchial plume movements [28], responses that are probably the result of the variability of energy requirements for their symbionts (e.g. sulfide or/and methane concentrations and oxygen availability) [4].

In addition to ocean tides, atmospheric forcing such as that brought by storms can have a strong influence on surface ocean dynamics, but only a few studies have considered its influence in the vent environment [29,30]. Winter storms affect near-bottom currents by generating downward-propagating inertial waves and low-frequency currents generated by pressure fluctuations associated with storm occurrence [31,32]. The large inertial oscillations generated by atmospheric forcing in the surface ocean appear to affect the dynamics of hydrothermal plumes at one vent site on the Juan de Fuca Ridge [29]. This surface-related influence is attributed to the presence of inertial oscillations in the surrounding currents. Variability in bottom currents at the Lucky Strike and Rainbow vent fields (Mid-Atlantic Ridge) appears to be influenced by inertial oscillations, whose period at this latitude is approximately 20 h [33]. Similarly, surface-generated mesoscale eddies appear to influence the transport of hydrothermal vent efflux and of vent larvae away from the northern East Pacific Rise [30]. Atmospheric forcing can therefore promote the spreading of hydrothermal effluents across the deep ocean and provide episodic opportunities for vent species to disperse their larvae over hundreds of kilometres.

Understanding precisely how environmental variability influences vent community dynamics is of particular relevance for hydrothermal biology. To date, only a few studies describing high-frequency variation in vent faunal behaviour have been published [28,34]. To establish whether tides play a role in vent species distributions, we monitored the variability of macrofaunal abundance in a *R. piscesae* assemblage from a northeast Pacific hydrothermal edifice at high temporal resolution. The recent development of deep-sea observatories facilitates high-resolution *in situ* studies of benthic communities [28,34–36]. Video imagery has proved to be appropriate for studying community dynamics and behaviour [36] as well as fine-scale changes in activity and faunal distribution [28,34]. Based on previous observations [28], we hypothesized that the fauna associated with *R. piscesae* tubeworms respond to the tidal signal through changes in food availability and environmental conditions. The objectives of this study were to (i) measure the environmental conditions possibly influenced by atmospheric and astronomic forcings, (ii) determine if species associated with the *R. piscesae* assemblage respond to these forces and (iii) assess changes in species activity in relation to variation in environmental conditions.

2. Material and methods

(a) Endeavour observatory

The 90-km Endeavour segment located on the northern part of the Juan de Fuca Ridge (JdFR) is a hydrothermally active region characterized by a 500–1000 m wide axial valley whose walls reach up to 200 m in height, and hosts five major hydrothermal vent fields. Within the Main Endeavour Field (MEF) (figure 1*a*), Grotto (47°56.958′ N, 129°5.899′ W) is an active hydrothermal sulfide vent cluster located at 2196 m depth covering 450 m^2 in surface area and 10 m high, forming a cove with an opening to the north (figure 1*b*). This edifice is characterized by high short-term variations in heat fluxes, but relative long-term stability (annual scale) [37]. As on many sulfide structures within the MEF, the site is colonized by a mosaic of faunal assemblages [38], including low-flow *Ridgeia piscesae* tubeworm assemblages and their associated fauna. Grotto was the subject of several scientific investigations, including the deployment of observational and measuring instruments by Ocean Networks Canada (ONC, figure 1*c*).

With a 25-year lifespan, the ONC's NEPTUNE-Canada subsea infrastructure rests on an 800 km loop of electric and fibre-optic cables connected to various instrumented sites (nodes). The Endeavour node includes an extension cable to the Grotto edifice instrument platform which supports a wide range of multidisciplinary sensors (figure 1*c*). Focused on vent ecology, the TEMPO-mini [39] ecological observatory module is deployed on the north slope of the edifice (figure 1*c*). The module is equipped with four 20 W LEDs lights and an Axis Q1755 camera featuring a 1/30 Progressive Scan CMOS 2 Megapixel image sensor, which recorded videos with a resolution of 1440 × 1080 pixels and a frame rate of 24 fps. A localized microchloration system protects sensor optical parts and projectors from biofouling [40].

(b) Environmental characterization

To study the impact of hydrodynamic patterns linked to ocean tides and surface storms on the hydrothermal abiotic habitat, we used temporal time series of physical and chemical variables acquired by instruments installed on or near the Grotto edifice (figure 1*c*; electronic supplementary material, table S1).

Pressure and near-bottom currents were measured with a highly sensitive bottom pressure recorder (BPR) and a 600 kHz acoustic Doppler current meter (ADCP). The ADCP had a useful vertical range of 30 m, and was located 70 m south of Grotto. Temperatures were measured by: (i) a 25 cm long thermocouple wand (BARS) inserted into a vigorously venting black-smoker orifice located 10 m west of TEMPO-mini, (ii) 12 autonomous temperature loggers (F-probes; F1–F12) placed on the tubeworm assemblage filmed by TEMPO-mini, (iii) an Aanderaa oxygen sensor deployed approximately 30 cm below the field of view, and (iv) a probe located under a fluid-collection

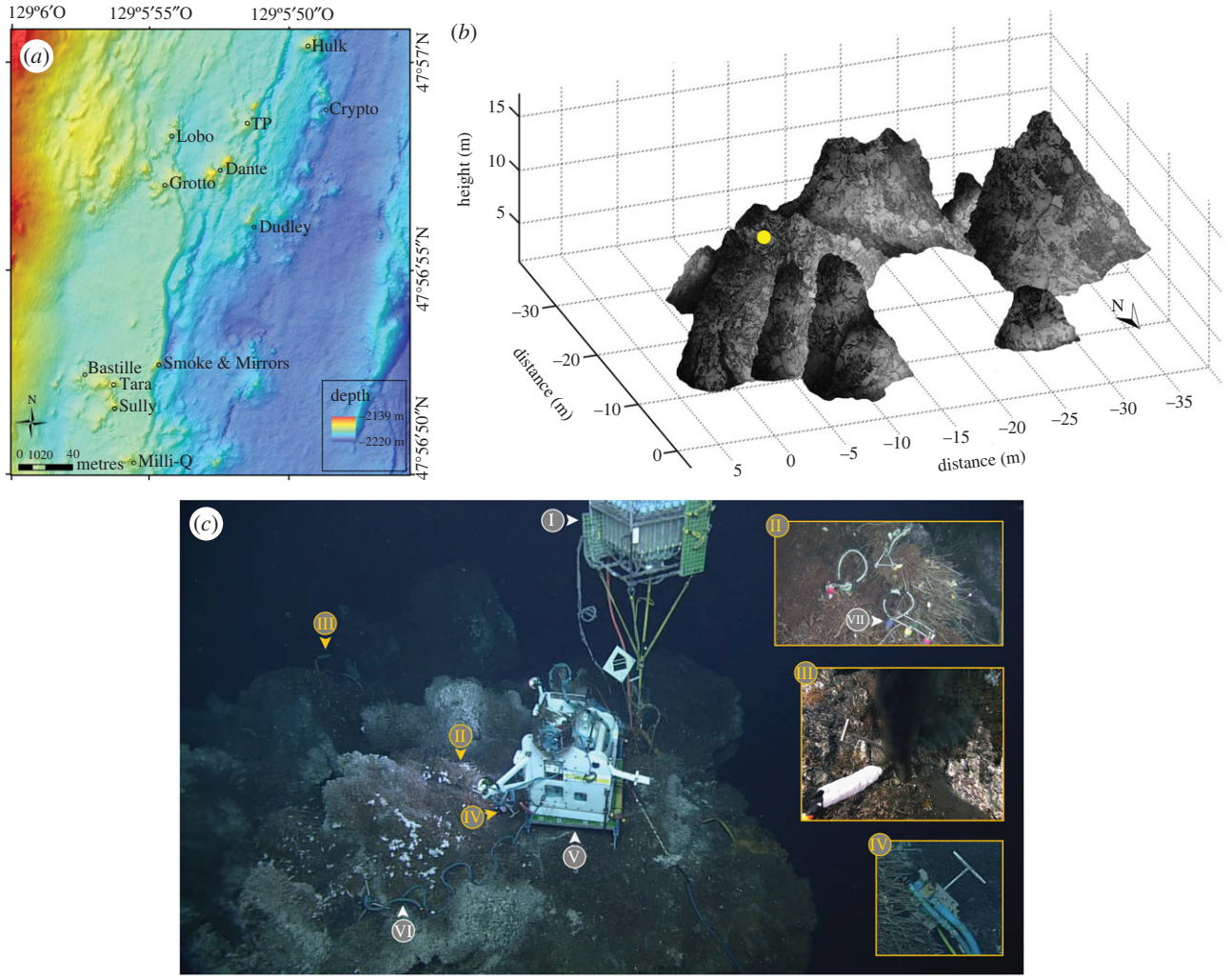

Figure 1. (*a*) Location map of the Main Endeavour Field (Juan de Fuca Ridge, northeast Pacific) indicating the positions of hydrothermal vent edifices, with (*b*) a visualization of the three-dimensional topographic structure of Grotto. The yellow dot on Grotto represents the position of TEMPO-mini. The distances and heights were estimated using COVIS (Cabled Observatory Vent-Imaging Sonar). (*c*) Deployed instruments: I = remote access sampler (RAS); II = assemblage filmed by the camera; III = benthic and resistivity sensors (BARS); IV = Aanderaa optode; V = TEMPO-mini; VI = thermistor chain (T-chain) and VII = autonomous temperature loggers (F-probes).

benthic chamber of the remote access fluid sampler (RAS) from a nearby (approx. 1.5 m) diffuse venting area. Oxygen saturation was measured with the Aanderaa optode.

Like many other studies on hydrothermal diffuse-flow habitats, we used temperature as a proxy measurement of chemical variability in the hydrothermal abiotic environment [3,4,13,41]. Increasing temperatures correspond to lesser dilution of vent fluids and therefore, suggest a high concentration of hydrogen sulfide, methane, metals and other reduced chemicals, as well as low-oxygen availability for communities.

(c) Observation design

To study long-term temporal dynamics of vent communities, the camera was programmed to record 20-min video sequences six times a day (02.00, 06.00, 10.00, 14.00, 18.00 and 22.00 UTC) with three zoom levels per sequence corresponding to 'large', 'medium' and 'fine' views. The camera was focused on a *Ridgeia piscesae* tubeworm assemblage harbouring a dense community of associated fauna (figure 2). The total studied surface covers approximately 0.315 m^2. Temporal variation in the observed abundances of four visible taxa (Ammotheidae pycnogonids, Polynoidae polychaetes, Buccinidae gastropods and Zoarcidae eelpouts) was quantified using the large and medium views (figure 2). To avoid 'observer bias' among consecutive measurements, video sequences were analysed in random order. The first observation strategy had a fixed daily observation time set at 10.00 UTC encompassing a year from 20 June 2013 to 20 June 2014. The second observation strategy was designed to identify seasonal components of macrofaunal and environmental variability. All six observations were analysed during one summer (June 2014) and two winters (November and December 2014) months. These specific time windows were selected to minimize the amount of missing data generated by temporary shortcomings of the observatory and to maximize the presence of high-quality video imagery.

(d) Statistical methods

All environmental variables were examined using two types of time-series analyses. Welch's averaged modified periodogram method [42,43] was used to identify the dominant periods, and tidal harmonic analyses using the open-source program T-TIDE [44] were used to assess the timing (phase of the cycles) and the degree to which the periodicities were determined by tidal forcing. Prior to analysis, the two-dimensional currents were rotated into components along and across the axis of the ridge. The spectra of the currents from 14 depths, ranging from 4 m to 30 m above the bottom, were examined.

Macrofaunal observed abundance time series were submitted to Dutilleul multi-frequential periodogram analysis (MFPA) to identify the dominant periods [45]. This periodogram computes

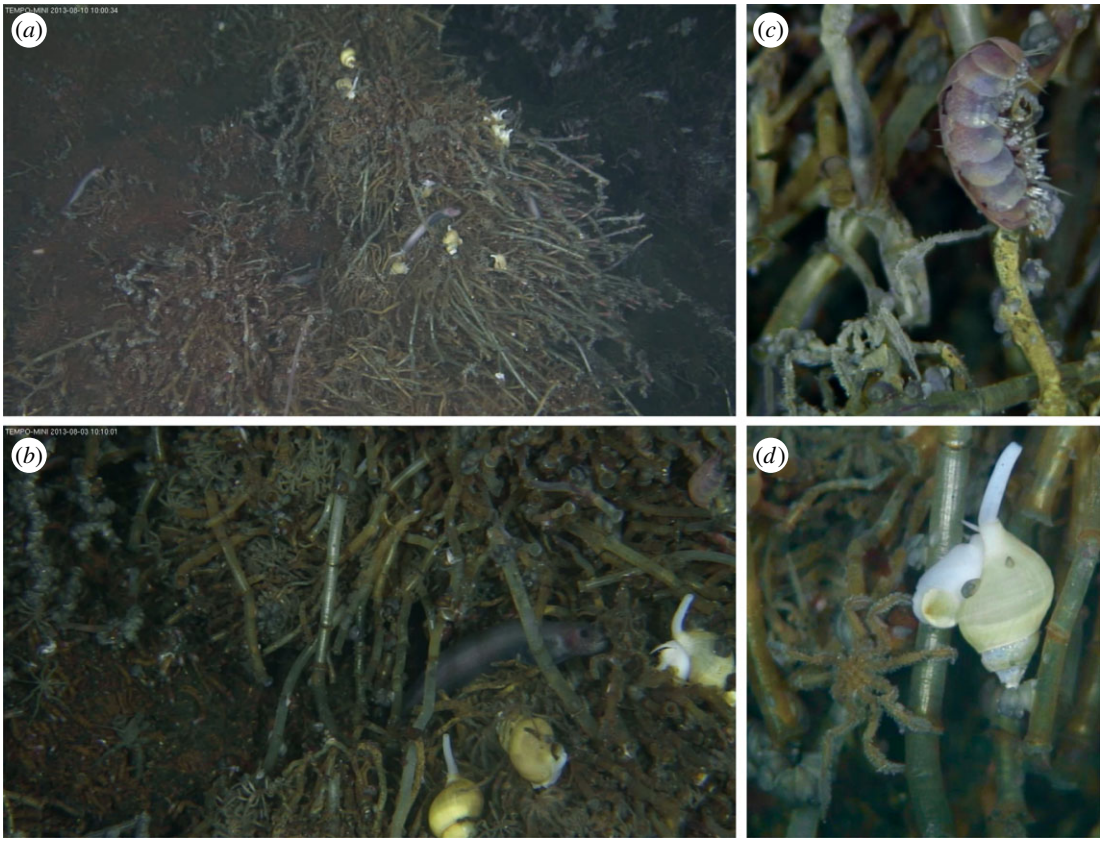

Figure 2. The *Ridgeia piscesae* tubeworms assemblage and associated fauna as viewed by the TEMPO-mini ecological observatory module at 2196 m depth at the Grotto hydrothermal edifice (Main Endeavour Field, JdFR), with (*a*) large and (*b*) medium views. (*c*) *Sericosura* sp. pycnogonids and Polynoidae polychaetes (*Branchinotogluma tunnicliffae*, *Lepidonotopodium piscesae* or *Levensteiniella kincaidi*) and (*d*) *Sericosura* sp. and the Buccinidae *Buccinum thermophilum* on the tubeworm assemblage.

the variance of periods that may or may not correspond to an integer number of cycles (fractional frequencies), by regression on the sinusoidal representation of the considered frequencies. The statistic of Dutilleul's periodogram is defined as the fraction of the total variance of the time series explained by regressing the series on the cosine and sine corresponding to a considered frequency; *p*-values are produced. Prior to analysis, missing values were substituted using a *k*-nearest neighbour method.

To investigate the processes of ocean dynamics that affect the variability of the observed abundances of macrofauna, path analyses [46] were performed using the program *Piste 3.2.1* (Legendre laboratory). To obtain parsimonious path models, variables were selected using a forward selection procedure (9999 permutations). Therefore, path models were divided into three compartments: (i) hydrodynamic processes defined by axial currents; (ii) the degree of mixing of seawater and hydrothermal fluids, represented by temperature and oxygen saturation; and (iii) macrofaunal abundance. The models were computed separately for the June, November and December 2014 data and only for vent species showing relationships with physical forcings. The observations of the Buccinidae *Buccinum thermophilum* and the Zoarcidae *Pachycara gymnium* were too scarce to allow modelling.

3. Results and discussion

(a) Ocean and hydrothermal ecosystem dynamics

The spectral analysis showed that bottom pressure was dominated by peaks in energy centred on the diurnal (24.8 h) and semidiurnal tidal bands (12.4 h), near frequencies of 1 and 2 cycles per day (electronic supplementary material, figure S1). The ratio of energy between the near-semidiurnal and near-diurnal bands matched those of barotropic tidal models of the northeast Pacific [47,48] with the near-semidiurnal band being about twice as energetic as the near-diurnal. Similarly, the dominant peaks in the current spectra were in the diurnal and semidiurnal bands, with the near-semidiurnal band being five times more energetic than the near-diurnal band (electronic supplementary material, figure S1). Harmonic analyses of the pressure and current time series revealed that the tidal constituents accounted for 99% and 31% of the variance, respectively.

Spectral analyses showed that periodicities in pressure and currents on Grotto occur at different frequency bands corresponding to distinct physical forcing mechanisms. First, the main near-semidiurnal band included the principal lunar semidiurnal M_2 and the principal solar semidiurnal S_2 tidal constituents, with periods of 12.42 h and 12 h, respectively (electronic supplementary material, figure S1). Tidal constituent M_2 had three times the amplitude of the second dominant constituent S_2. As shown in other studies, the semidiurnal frequency dominates tidal oscillations in the deep currents of the Endeavour axial valley [16,49]. Interestingly, the semidiurnal energy was almost entirely concentrated in the along-valley axis component and greatly diminished in the weak cross-axis component (data not shown). Second, the diurnal band resulted from the lunar diurnal K_1 and the solar diurnal P_1 tidal constituents, with periods of 23.93 and 24.07 h (electronic supplementary material, figure S1), respectively, and differing by a factor of 2.5. Finally, the enhanced energy peak with a period in

Table 1. Observed abundances and significant results of Dutilleul periodogram analysis of the hydrothermal vent fauna at the Grotto edifice (2196 m depth). The data were obtained by visual analysis of the video images recorded by TEMPO-mini during a whole year (once a day) and during three selected months (six times a day).

	annual analysis		monthly analyses					
	20 June 2013 to 20 June 2014		June 2014		November 2014		December 2014	
taxa	min–max (mean ± s.d.)	main periods	min–max (mean ± s.d.)	main periods	min–max (mean ± s.d.)	main periods	min–max (mean ± s.d.)	main periods
Sericosura sp.	2–31 (14.7 ± 5.85)	14.89-d	14–46 (24.32 ± 5.62)	12.39 h	15–48 (26.75 ± 5.57)	4.07-d 12.43 h	9–37 (23.65 ± 5.36)	4.24-d 12.42 h
Polynoidae	1–34 (8.57 ± 3.53)	—	4–20 (10.81 ± 3.47)	—	7–24 (14.68 ± 3.6)	16.03-h	7–25 (14.36 ± 3.86)	12.39 h

the range of 3–4 days and at higher nonlinear harmonics of the tidal frequencies (electronic supplementary material, figure S1). Four-day oscillations in current measurements have been widely observed over the JdFR [17,50] and seem to be related to atmospheric forcing [51].

The spectra of temperatures (F-probes) and oxygen saturation from a diffuse venting area also revealed significant peaks at the near-semidiurnal and near-diurnal frequencies (electronic supplementary material, figure S1). Tidal modulation of diffuse-flow vent temperatures has been previously reported at JdFR [14,52] and has also been observed in records from a thermistor chain associated with TEMPO-mini, deployed near the studied community [28] (figure 1*c*). These tidal peaks had less power than those of the pressure and current spectra. Tidal oscillations were more episodic and less persistent in diffuse fluids than in the high-temperature black-smoker fluids, where tidal oscillations were steadier and comparable with the pressure record. This result may be explained by the fact that high-temperature black-smoker data were acquired by a probe inserted into the chimney orifice and, therefore, protected from the influence of near-bottom currents. By contrast, temperature data from diffuse-flow areas were exposed to bottom currents, thereby masking the tidal signal.

The potential mechanisms causing this tide-related variability on the hydrothermal abiotic environment include oceanic tidal pressure and modulation of horizontal bottom currents by ocean tides. Barreyre *et al*. [20] have reported that tidal variability in high-temperature black-smoker fluids was significantly more coherent with tidal pressure, while diffuse-flow vent temperatures were more coherent with tidal currents. These ambient currents and their hydrodynamic oscillations have a complex, but direct implication on the dispersal of hydrothermal effluents and influence temperature variability [15,21], suggesting a high variability of chemical conditions in the hydrothermal ecosystem [41,53]. In the Endeavour axial valley, where the dominant along-axis periodicity of ambient currents is tidal, ocean tides probably have a strong effect on the environment surrounding the faunal community. In our video sequences, we observed evident changes in environmental conditions with alternation between 'clear' seawater and shimmering fluids characteristics of diffuse venting (electronic supplementary material, video S1).

(b) Tides and vent faunal dynamics

Located near a hydrothermal diffuse area, the *Ridgeia piscesae* tubeworms assemblage filmed by TEMPO-mini was recognized as a 'V low-flow' community [38]. In light of previous knowledge on JdFR species diversity, we identified the ammotheid pycnogonids as *Sericosura* sp. Given three morphologically similar species of *Sericosura* have been described from the Endeavour segment of the JdFR [Bamber 2009], we refrained from assigning the pycnogonids to a single species. In contrast, it was possible to assign polynoid polychaetes to three species including *Branchinotogluma tunnicliffae*, *Lepidonotopodium piscesae* and *Levensteiniella kincaidi*.

Dutilleul's periodograms computed on 1 year of simulated data containing a tidal signal showed that, with one observation per day, a cosine with 12.42 h tidal period sampled once a day produced a significant 14.79-day harmonic. A 14.89-day period was detected in the periodogram of *Sericosura* sp. abundances observed during 1 year (table 1), highlighting a tidal signal. For the June, November and December 2014 time series, periodograms displayed a significant approx. 12.4 h period corresponding to the semidiurnal tidal cycle (table 1). The observed abundances of Polynoidae at the top of the *Ridgeia* bush exhibited a significant tidal cycle (12.4 h) in the December data only (table 1).

To deepen our understanding of tide-related variables on the behaviour of the two taxa that displayed significant tidal signals, we decomposed their linear effects on the temporal dynamics of vent species using path analyses performed on one-month observation periods (figure 3). Tidal pressure was not retained in our path models, suggesting that the temporal dynamics of the studied vent taxa is mainly controlled by a mechanism related to tidal bottom currents. This result is in agreement with Barreyre *et al*. [20], which shows that diffuse-flow vent environments are mainly affected by tidal bottom currents. Consistent with the main orientation of the ridge and the topography of Grotto (electronic supplementary material, figure S2), path models showed that temperature and oxygen saturation in the tubeworm's environment were strongly and significantly influenced by the northern and southern horizontal bottom tidal currents (along the valley axis). The horseshoe-shaped hydrothermal cluster is open on the northeast side, directly exposed to the north–south current axis (figure 1*b*). The height of the

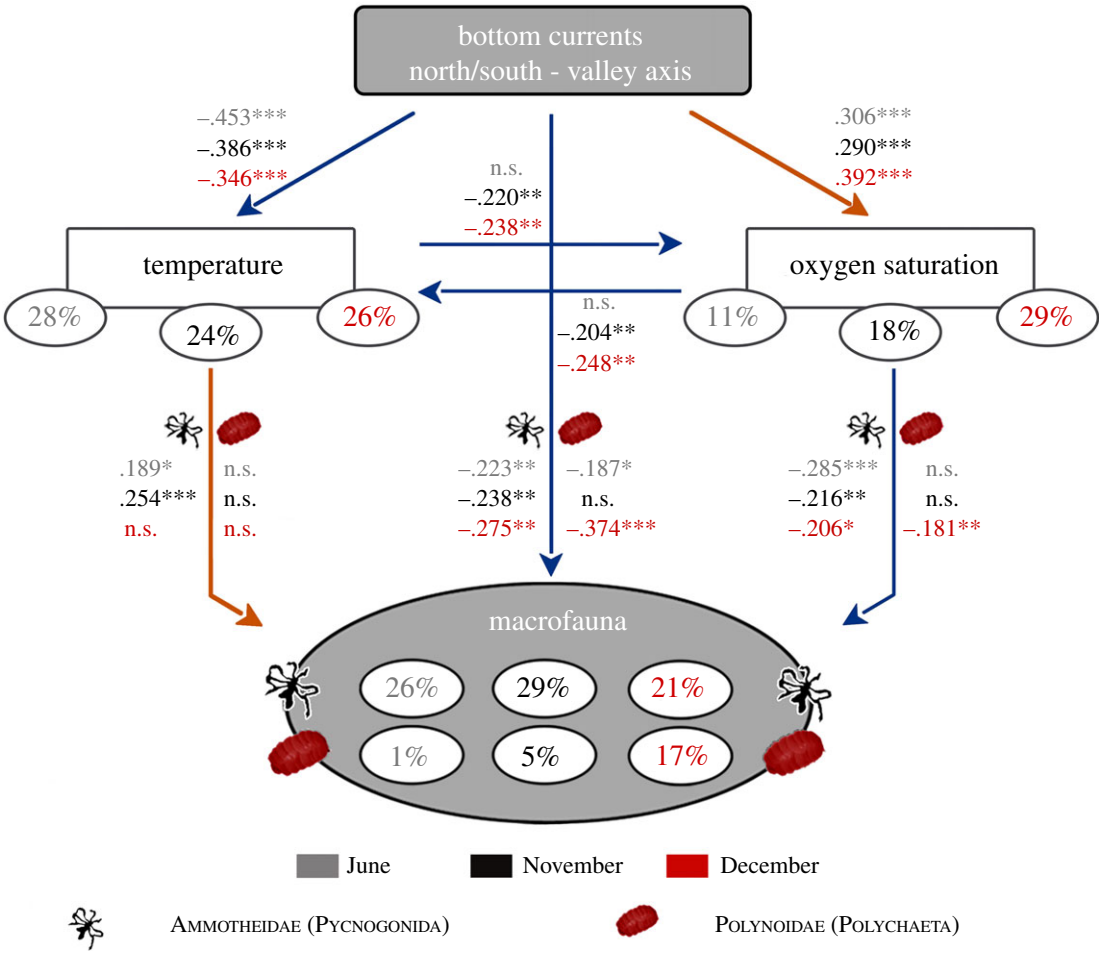

Figure 3. Path analysis model of ocean tide effects on Ammotheidae pycnogonids *Sericosura* sp. and Polynoidae polychaetes abundances in one summer (June 2014) and two winter (November and December 2014) months. Orange arrows indicate positive relationships, blue arrows negative relationships. Path coefficients indicate the direct relationships between the variables. Significance codes: not significant (n.s.), (*) $p \leq 0.05$, (**) $p \leq 0.01$ and (***) $p \leq 0.001$. Indirect effects were estimated by multiplying the coefficients of individual segments along paths. The percentages shown in ellipses indicate the proportion of variance explained by the model (adjusted R^2).

northern towers (10 m) may further protect the studied assemblage from east–west currents, not retained in path models. Hydrodynamic processes lead to an alternating regime of abiotic conditions. During southern current phases (directed towards the north), the environment of the siboglinids was characterized by low temperatures and high oxygen saturation (figure 3). Conversely, northern current phases (directed towards the south) were associated with high temperatures and low-oxygen saturation (figure 3), suggesting high inputs of hydrothermal fluids in the tubeworm habitat. High temperatures indicate high concentrations of hydrothermal fluids, therefore high concentrations of hydrogen sulfide and other reduced chemicals in the ambient habitat of the tubeworm assemblage [3,4,12,13].

Path models revealed that observed macrofaunal abundances (at the top of the bush) decreased during low temperature (positive path coefficients) and high oxygen saturation conditions (negative path coefficients; figure 3). We hypothesize that, in these local favourable conditions (i.e. lower toxicity), species remain deeper in the tubeworm bush (figure 4), protecting themselves against currents and predation, and possibly allocating their energy to nutrition and/or reproduction. Individuals within the bush were not visible to the observer, reducing the number of counted individuals. In the reverse conditions, we postulate that the high concentration of hydrothermal fluids in the environment prompted the vent species to reach the surface of the tubeworms (figure 4) in search of more favourable habitat conditions than inside the bush, such as higher oxygen saturation. This behaviour would then lead to a higher number of individuals, visible at the top of the bush.

Aggregation (defined as a group of more than five individuals) at the top of tubeworms and enhanced activity of pycnogonids occurred during high-temperature and low-oxygen saturation periods. This behavioural observation may be associated with respiration. In the absence of a respiratory system and pigments that can transport oxygen, pycnogonids breathe by diffusion through their chitinous exoskeleton [54]. Because their cardiac system is too weak to circulate haemolymph [55], leg joint and peristaltic movements exert pressure on haemolymph, allowing oxygen transport [54,56]. Oxygen consumption varies not only with their activity levels, but also with the contact between individuals [57]. Pycnogonid respiration appears to be greater when they are in groups than when they are isolated [57]. This would explain the aggregations observed in periods of relatively low-oxygen availability. In this study, oxygen saturations varied from 1.5 to 22%. Following Woods *et al.* [58], these levels of oxygen represent low species tolerance. Interestingly in the Antarctic, several species of genus *Ammothea*, a close relative of *Sericosura*, also supports low levels of oxygen, suggesting an evolutionary history of wider dissolved oxygen range in at least some ammotheids, which

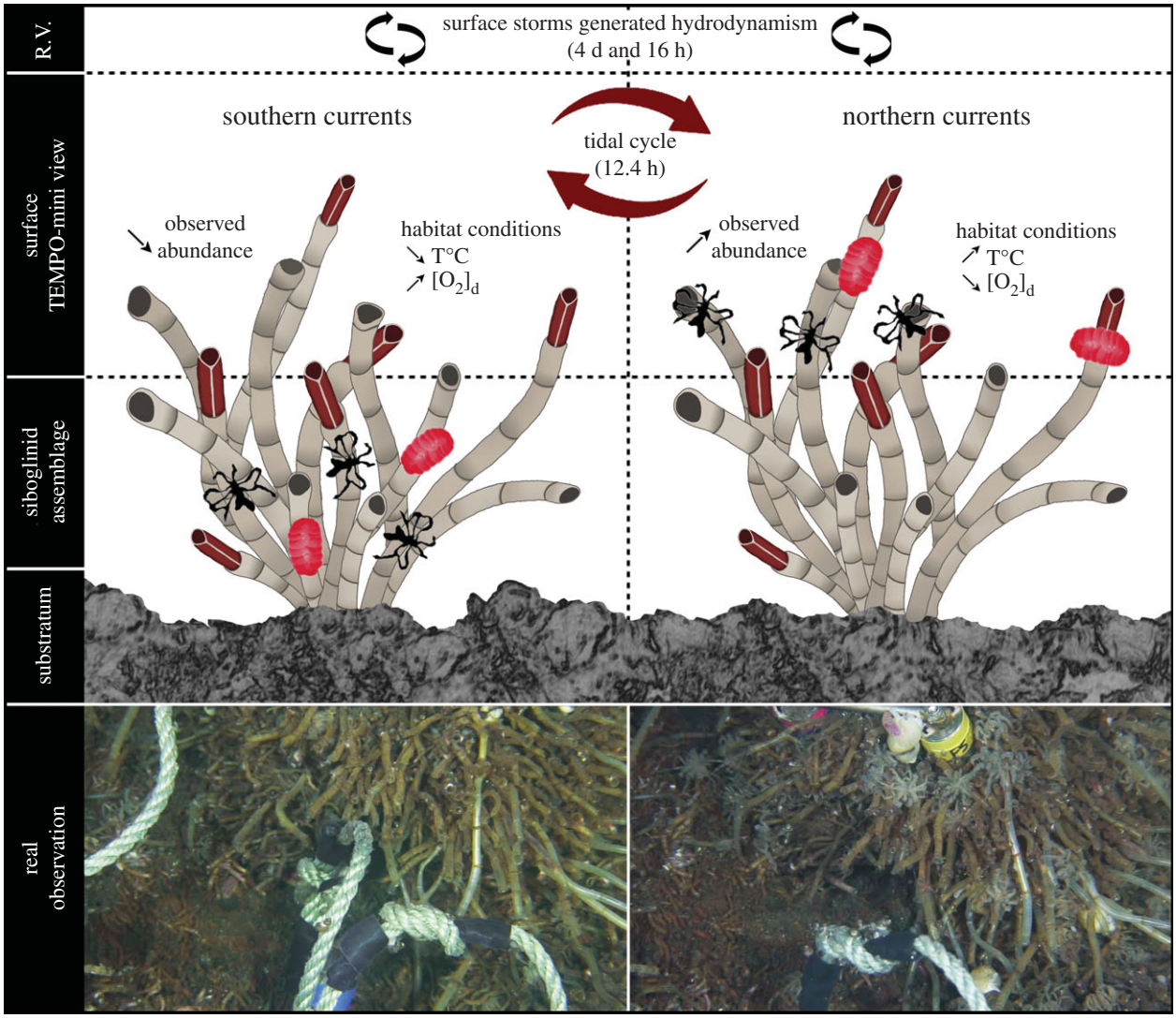

Figure 4. Schematic representation of the influence of ocean tides and local surface storms on the hydrothermal abiotic environment and vent species' dynamics, associated with real observation. Oscillatory currents affect the balance between hydrothermal fluid inputs and the surrounding seawater, modifying the physical and chemical conditions of the vent habitat. Hydrothermal species react to these habitat modifications by adjusting their behaviour, e.g. by moving up and down the tubeworm assemblage. The left and right sides represent the two states observed in relation to the tides. The horizontal dashed lines separate the different compartments from the Ridge Valley (R.V.) at the top, the surface of the bush (area visible with TEMPO-mini) in the middle and within the bush (invisible to the human eye) at the bottom.

relates well with the dominance of species of *Sericosura* in chemosynthetic, hypoxic environments.

Polynoidae showed no distinctive patterns in abundance with respect to temperature variability (figure 3). Laboratory experiments in pressurized aquaria have shown that hydrothermal polynoids tolerate a wide range of thermal conditions, with an activity recorded from 2.5 to 23°C and thermal limits in the range of 35–40°C [59]. Here, temperatures experienced by the organisms as measured by the F-probes in the field of view ranged between 1.6°C and 13.6°C. The absence of significant influence of temperature on their abundances corroborates with these previous findings and suggests that polynoids are in their optimal niche. In contrast with littoral species, the presence of gills and haemoglobin with high oxygen affinity in vent polynoids promotes oxygen uptake in hypoxic environments. However, in December 2014, the abundance pattern of polynoids followed a tidal signal (table 1). Near-bottom currents may modulate the availability of food or/and other unmeasured environmental variables, but the detection of this signal only in December remains to be investigated.

(c) Surface storms and deep-sea fauna

Many studies have shown an influence of surface storms on near-bottom currents and their repercussions on hydrothermal abiotic environments [17,31,50,60]. However, the effects of atmospheric forcing on vent fauna were poorly explored [30]. Dutilleul's periodograms computed for November show that the observed abundances of pycnogonids and polynoids responded to local atmospheric forcing with an approximately 4-day oscillation and 16-h inertial oscillation, respectively, possibly related to surface storms (table 1). Similarly in December, observed abundances of pycnogonids responded to a signal corresponding possibly to local atmospheric forcing with an approximately 4-day oscillation (table 1).

The Rossby wave-like nature of winter storms at mid-latitudes imparts a 3–4 day cycle in atmospheric pressure due to the passage of alternating high and low pressure systems. This pressure oscillation has been known to set up bottom-trapped waves on the flanks of the JdFR. Spectra from our pressure and current records (electronic supplementary material, figure S1) show evidence of a 4-day peak as

previously reported [17,31,50,51]. An earlier study reported amplification of the 4-day energy during winter and coherence between local wind stress and 4-day periods in currents, supporting storm-induced generation [51]. In contrast with the inertial motions, 4-day energy is maximal in the Endeavour axial valley, where inertial wave energy cannot propagate [51]. As suggested by Cannon & Thomson [17], the 4-day oscillation may have an important implication on the local advection of hydrothermal effluents, periodically inducing changes in habitat conditions and vent species' responses to abiotic constraints and/or food availability. A 4.5 day cycle in buccinid abundance was observed by Cuvelier *et al*. [28], but no abiotic data were reported.

At the latitude of Grotto, the 16-h period found in observed polychaete abundances corresponds to that of wind-generated inertial currents [31,61]. Induction of these episodic inertial motions may be caused by the passage of storms. When winds at the sea surface are weak or absent, previously induced water movements trace inertial circles because of the Coriolis effect due to the Earth's rotation. This inertial period was previously observed in October 2010 in a Grotto hydrothermal flux time series, showing that surface winter storms influence hydrothermal plume dynamics [29]. However, the environmental variable spectra (electronic supplementary material, figure S1) within the axial valley did not reveal significant energy at the 16-h inertial period. Thomson *et al*. [31] reported that inertial motions are the most energetic component of the flow variability in the vicinity of Endeavour during the winter season, except within the axial valley. The narrowness and small size of the rift valley may not permit entry of internal inertial waves, which are large and propagate at a very small (less than 2°) angle to the horizontal plane. Conversely, these inertial waves are enhanced above the ridge (approx. 200 mab) where vent plumes of the MEF rise to a level of neutral buoyancy at 50–350 mab [16]. These inertial motions may periodically contribute to the advection of hydrothermal flow, resident particles and chemical components.

The 4-day oscillation and 16-h inertial period may influence vent species dynamics, by modifying the periodic variability of local environmental conditions and particles settling from the hydrothermal plumes (figure 4). For example, surface-generated mesoscale eddies were observed to influence the transport of hydrothermal vent efflux and vent larvae away from the ridge [30]. The addition of sediment traps could help validate this hypothesis. This evidence of the influence of surface storms on vent species' dynamics emphasizes the need to deepen our understanding of the impacts of atmospheric forcing on hydrothermal ecosystems.

4. Conclusion and perspectives

Our results strongly demonstrate that global ocean dynamics significantly influence the functioning of hydrothermal ecosystems. To our knowledge, this is the first study showing that ocean tides and winter surface storms influence the dynamics of benthic non-symbiotic hydrothermal vent species. Deep-sea currents generate different regimes of abiotic conditions within *Ridgeia piscesae* assemblages and associated fauna. Alternating periods of high and low hydrothermal fluid inputs trigger temporal variability in vent species by possibly modulating their activity and behaviour in search of optimal conditions. An alternative explanation assumes that vent fauna harbour endogenous timekeeping mechanisms, the so-called biological clock. Encoded by clock genes, biological rhythms are phylogenetically constrained without necessarily being linked to existing cyclic environmental signals. These rhythms may constitute an anticipated response of organisms to changing environmental conditions caused by ocean variability. Possibly related to these internal biological rhythms, Colaço *et al*. [62] reported that vent mussels *Bathymodiolus azoricus* spawned annually, in January, both in controlled aquaria conditions at atmospheric pressure and in the wild population. Our results call therefore for experimental studies to investigate this assumption by using pressurized aquaria or molecular approaches to identify the presence of active clock genes in the vent fauna.

Data accessibility. The raw data used in this research have been made publicly available on Ocean Networks Canada website: http://www.oceannetworks.ca.

Authors' contributions. P.-M.S., J.S. and R.W.L. designed the research project and developed the instrumentation. Y.L., P.L., M.M., S.M. P.-M.S. and J.S. conceived the ideas and contributed to the interpretation of the results. Y.L., P.L. and S.M. analysed data. C.P.A. contributed to pycnogonid identification and interpretation of pycnogonid data. P.L., M.M. and J.S. supervised the research project. All authors contributed to the writing process and revised the manuscript.

Competing interests. We have no competing interests.

Funding. This research was supported by Ifremer budget, and a NSERC research grant to P.L. and a grant from the 'Laboratoire d'Excellence' LabexMER (ANR-10-LABX-19). This work was co-funded by a grant from the French government under the programme 'Investissements d'avenir'.

Acknowledgements. The authors thank the engineers and technicians who developed and maintain TEMPO-mini (Ifremer RDT, LEP, ONC). Extended thanks go to the captain and crews of the R/V Thomas G. Thompson, the staff of ONC and ROVs ROPOS and Oceaneering Millennium® during the deployment and recovery cruises. We are grateful to all PIs of ONC for accessing their temporal data. We are also grateful to M. Lelièvre, and the Québec Centre for Biodiversity Science.

References

1. Lonsdale P. 1977 Clustering of suspension-feeding macrobenthos near abyssal hydrothermal vents at oceanic spreading centers. *Deep. Res. Part I Oceanogr. Res. Pap.* **24**, 857–863.
2. Tunnicliffe V. 1991 The biology of hydrothermal vents: ecology and evolution. *Oceanogr. Mar. Biol. Annu. Rev.* **29**, 319–407.
3. Sarradin P-M, Caprais J-C, Briand P, Gaill F, Shillito B, Desbruyères D. 1998 Chemical and thermal description of the Genesis hydrothermal vent community environment (13°N, EPR). *Cah. Biol. Mar.* **39**, 159–167.
4. Childress JJ, Fisher CR. 1992 The biology of hydrothermal vent animals: physiology, biochemistry, and autotrophic symbioses. *Oceanogr. Mar. Biol. Annu. Rev.* **30**, 337–441.
5. Sarrazin J, Juniper SK, Massoth G, Legendre P. 1999 Physical and chemical factors influencing species distributions on hydrothermal sulfide edifices of the Juan de Fuca Ridge, northeast Pacific. *Mar. Ecol. Prog. Ser.* **190**, 89–112. (doi:10.3354/meps190089)

6. Levesque C, Juniper SK, Marcus J. 2003 Food resource partitioning and competition among alvinellid polychaetes of Juan de Fuca Ridge hydrothermal vents. *Mar. Ecol. Prog. Ser*. **246**, 173–182. (doi:10.3354/meps246173)
7. De Busserolles F, Sarrazin J, Gauthier O, Gélinas Y, Fabri M-C, Sarradin P-M, Desbruyères D. 2009 Are spatial variations in the diets of hydrothermal fauna linked to local environmental conditions? *Deep. Res. Part II Top. Stud. Oceanogr*. **56**, 1649–1664. (doi:10.1016/j.dsr2.2009.05.011)
8. Micheli F, Peterson CH, Mullineaux LS, Fisher CR, Mills SW, Sancho G, Johnson GA, Lenihan HS. 2002 Predation structures communities at deep-sea hydrothermal vents. *Ecol. Monogr*. **72**, 365–382. (doi:10.1890/0012-9615(2002)072[0365:PSCADS]2.0.CO;2)
9. Mullineaux LS, Peterson CH, Micheli F, Mills SW. 2003 Successional mechanism varies along a gradient in hydrothermal fluid flux at deep-sea vents. *Ecol. Monogr*. **73**, 523–542. (doi:10.1890/02-0674)
10. Tunnicliffe V, Embley RW, Holden JF, Butterfield DA, Massoth GJ, Juniper SK. 1997 Biological colonization of new hydrothermal vents following an eruption on Juan de Fuca Ridge. *Deep. Res. Part I Oceanogr. Res. Pap*. **44**, 1627–1644. (doi:10.1016/S0967-0637(97)00041-1)
11. Crone TJ, Wilcock WSD, McDuff RE. 2010 Flow rate perturbations in a black smoker hydrothermal vent in response to a mid-ocean ridge earthquake swarm. *Geochemistry, Geophys. Geosystems* **11**, 1–13. (doi:10.1029/2009GC002926)
12. Johnson KS, Beehler CL, Sakamoto-Arnold CM, Childress JJ. 1986 *In situ* measurements of chemical distributions in a deep-sea hydrothermal vent field. *Science*. **231**, 1139–1141. (doi:10.1126/science.231.4742.1139)
13. Johnson KS, Childress JJ, Hessler RR, Sakamoto-Arnold CM, Beehler CL. 1988 Chemical and biological interactions in the Rose Garden hydrothermal vent field, Galapagos spreading center. *Deep Sea Res. Part A. Oceanogr. Res. Pap*. **35**, 1723–1744. (doi:10.1016/0198-0149(88)90046-5)
14. Tivey M, Bradley A, Terrence J, Kadco D. 2002 Insights into tide-related variability at seafloor hydrothermal vents from time-series temperature measurements. *Earth Planet. Sci. Lett*. **202**, 693–707. (doi:10.1016/S0012-821X(02)00801-4)
15. Scheirer DS, Shank TM, Fornari DJ. 2006 Temperature variations at diffuse and focused flow hydrothermal vent sites along the northern East Pacific Rise. *Geochem. Geophys. Geosyst.* **7**, 1–23. (doi:10.1029/2005GC001094)
16. Thomson RE, Mihály SF, Rabinovich AB, McDuff RE, Veirs SR, Stahr FR. 2003 Constrained circulation at Endeavour ridge facilitates colonization by vent larvae. *Nature* **424**, 545–549. (doi:10.1038/nature01824)
17. Cannon GA, Thomson RE. 1996 Characteristics of 4-day oscillations trapped by the Juan de Fuca Ridge. *Geophys. Res. Lett*. **23**, 1613–1616. (doi:10.1029/96GL01370)
18. Connell JH. 1972 Community interactions on marine rocky intertidal shores. *Annu. Rev. Ecol. Syst*. **3**, 169–192. (doi:10.1146/annurev.es.03.110172.001125)
19. Kinoshita M, Von Herzen RP, Matsubayashi O, Fujioka K. 1998 Tidally-driven effluent detected by long-term temperature monitoring at the TAG hydrothermal mound, Mid-Atlantic Ridge. *Phys. Earth Planet. Inter*. **108**, 143–154. (doi:10.1016/S0031-9201(98)00092-2)
20. Barreyre T, Escartin J, Sohn RA, Cannat M, Ballu V, Crawford WC. 2014 Temporal variability and tidal modulation of hydrothermal exit-fluid temperatures at the Lucky Strike deep-sea vent field, Mid-Atlantic Ridge. *J. Geophys. Res. Solid Earth* **119**, 2543–2566. (doi:10.1002/2013JB010478)
21. Little SA, Stolzenbach KD, Grassle FJ. 1988 Tidal current effects on temperature in diffuse hydrothermal flow: Guaymas basin. *Geophys. Res. Lett*. **15**, 1491–1494. (doi:10.1029/GL015i013p01491)
22. Johnson KS, Childress JJ, Beehler CL, Sakamoto CM. 1994 Biogeochemistry of hydrothermal vent mussel communities: the deep-sea analogue to the intertidal zone. *Deep. Res. Part I Oceanogr. Res. Pap*. **41**, 993–1011. (doi:10.1016/0967-0637(94)90015-9)
23. Cosson RP, Thiébaut É, Company R, Castrec-Rouelle M, Colaço A, Martins I, Sarradin PM, Bebianno MJ. 2008 Spatial variation of metal bioaccumulation in the hydrothermal vent mussel *Bathymodiolus azoricus*. *Mar. Environ. Res*. **65**, 405–415. (doi:10.1016/j.marenvres.2008.01.005)
24. Charmasson S, Sarradin P-M, Le Faouder A, Agarande M, Loyen J, Desbruyères D. 2009 High levels of natural radioactivity in biota from deep-sea hydrothermal vents: a preliminary communication. *J. Environ. Radioact*. **100**, 522–526. (doi:10.1016/j.jenvrad.2009.02.002)
25. Schöne BR, Giere O. 2005 Growth increments and stable isotope variation in shells of the deep-sea hydrothermal vent bivalve mollusk *Bathymodiolus brevior* from the North Fiji Basin, Pacific Ocean. *Deep. Res. Part I Oceanogr. Res. Pap*. **52**, 1896–1910. (doi:10.1016/j.dsr.2005.06.003)
26. Nedoncelle K, Lartaud F, de Rafelis M, Boulila S, Le Bris N. 2013 A new method for high-resolution bivalve growth rate studies in hydrothermal environments. *Mar. Biol*. **160**, 1427–1439. (doi:10.1007/s00227-013-2195-7)
27. Nedoncelle K, Lartaud F, Contreira-Pereira L, Yücel M, Thurnherr AM, Mullineaux L, Le Bris N. 2015 *Bathymodiolus* growth dynamics in relation to environmental fluctuations in vent habitats. *Deep Sea Res. Part I Oceanogr. Res. Pap*. **106**, 183–193. (doi:10.1016/j.dsr.2015.10.003)
28. Cuvelier D, Legendre P, Laes A, Sarradin P-M, Sarrazin J. 2014 Rhythms and community dynamics of a hydrothermal tubeworm assemblage at Main Endeavour Field—a multidisciplinary deep-sea observatory approach. *PLoS ONE* **9**, e96924. (doi:10.1371/journal.pone.0096924)
29. Xu G, Jackson DR, Bemis KG, Rona PA. 2013 Observations of the volume flux of a seafloor hydrothermal plume using an acoustic imaging sonar. *Geochem. Geophys. Geosyst.* **14**, 2369–2382. (doi:10.1002/ggge.20177)
30. Adams DK, Mcgillicuddy Jr DJ, Zamudio L, Thurnherr AM, Liang X, Rouxel O, German CR, Mullineaux LS. 2011 Surface-generated mesoscale eddies transport deep-sea products from hydrothermal vents. *Science* **332**, 580–583. (doi:10.1126/science.1201066)
31. Thomson RE, Roth SE, Dymond J. 1990 Near-inertial motions over a mid-ocean ridge: effects of topography and hydrothermal plumes. *J. Geophys. Res*. **95**, 7261–7278. (doi:10.1029/JC095iC05p07261)
32. D'Asaro EA. 1995 Upper-ocean inertial currents forced by a strong storm. Part III: interaction of inertial currents and mesoscale eddies. *J. Phys. Oceanogr*. **25**, 2953–2958. (doi:10.1175/1520-0485(1995)025<2953:UOICFB>2.0.CO;2)
33. Khripounoff A, Vangriesheim A, Crassous P, Segonzac M, Lafon V, Warén A. 2008 Temporal variation of currents, particulate flux and organism supply at two deep-sea hydrothermal fields of the Azores Triple Junction. *Deep. Res. Part I Oceanogr. Res. Pap*. **55**, 532–551. (doi:10.1016/j.dsr.2008.01.001)
34. Sarrazin J, Cuvelier D, Peton L, Legendre P, Sarradin P-M. 2014 High-resolution dynamics of a deep-sea hydrothermal mussel assemblage monitored by the EMSO-Açores MoMAR observatory. *Deep. Res. Part I Oceanogr. Res. Pap*. **90**, 62–75. (doi:10.1016/j.dsr.2014.04.004)
35. Matabos M, Bui AOV, Mihály S, Aguzzi J, Juniper K, Ajayamohan RS. 2014 High-frequency study of epibenthic megafaunal community dynamics in Barkley Canyon: a multi-disciplinary approach using the NEPTUNE Canada network. *J. Mar. Syst*. **130**, 56–68. (doi:10.1016/j.jmarsys.2013.05.002)
36. Matabos M, Cuvelier D, Brouard J, Shillito B, Ravaux J, Zbinden M, Barthelemy D, Sarradin P-M, Sarrazin J. 2015 Behavioural study of two hydrothermal crustacean decapods: *Mirocaris fortunata* and *Segonzacia mesatlantica*, from the Lucky Strike vent field (Mid-Atlantic Ridge). *Deep Sea Res. Part II Top. Stud. Oceanogr*. **121**, 146–158.
37. Xu G, Jackson DR, Bemis KG, Rona PA. 2014 Time-series measurement of hydrothermal heat flux at the Grotto mound, Endeavour Segment, Juan de Fuca Ridge. *Earth Planet. Sci. Lett*. **404**, 220–231. (doi:10.1016/j.epsl.2014.07.040)
38. Sarrazin J, Robigou V, Juniper SK, Delaney JR. 1997 Biological and geological dynamics over four years on a high-temperature sulfide structure at the Juan de Fuca Ridge hydrothermal observatory. *Mar. Ecol. Prog. Ser*. **153**, 5–24. (doi:10.3354/meps153005)
39. Auffret Y *et al.* 2009 TEMPO-mini: a custom-designed instrument for real-time monitpring of hydrothermal vent ecosystems. *Instrum. Viewp*. **8**, 17.

40. Delauney L, Compare C, Lehaitre M. 2010 Biofouling protection for marine environmental sensors. *Ocean Sci*. **6**, 503–511. (doi:10.5194/os-6-503-2010)
41. Le Bris N, Rodier P, Sarradin P-M, Le Gall C. 2006 Is temperature a good proxy for sulfide in hydrothermal vent habitats? *Cah. Biol. Mar*. **47**, 465–470.
42. Welch PD. 1967 The use of fast Fourier transform for the estimation of power spectra: a method based on time averaging over short, modified periodograms. *IEEE Trans Audio* **AU-15**, 70–73.
43. Thomson RE, Emery WJ. 2014 *Data analysis methods in physical oceanography*. Waltham, MA: Elsevier Science.
44. Pawlowicz R, Beardsley B, Lentz S. 2002 Classical tidal harmonic analysis including werror estimates in MATLAB using T_TIDE. *Comput. Geosci*. **28**, 929–937. (doi:10.1016/S0098-3004(02)00013-4)
45. Dutilleul P. 2001 Multi-frequential periodogram analysis and the detection of periodic components in time series. *Commun. Stat. Theory Methods* **30**, 1063–1098. (doi:10.1081/STA-100104350)
46. Wright S. 1934 The method of path coefficients. *Ann. Math. Stat*. **5**, 161–215. (doi:10.1214/aoms/1177732676)
47. Flather RA. 1987 A tidal model of the northeast Pacific. *Atmos. Ocean* **25**, 22–45. (doi:10.1080/07055900.1987.9649262)
48. Foreman MGG, Crawford WR, Cherniawsky JY, Henry RF, Tarbotton MR. 2000 A high-resolution assimilating tidal model for the northeast Pacific Ocean. *J. Geophys. Res*. **105**, 28629. (doi:10.1029/1999JC000122)
49. Veirs SR, McDuff RE, Stahr FR. 2006 Magnitude and variance of near-bottom horizontal heat flux at the Main Endeavour hydrothermal vent field. *Geochem., Geophys. Geosyst*. **7**, 1–16, Q02004. (doi:10.1029/2005GC000952)
50. Cannon GA, Pashinski DJ. 1990 Circulation near Axial Seamount. *J. Geophys. Res. Solid Earth* **95**, 12 823–12 828. (doi:10.1029/JB095iB08p12823)
51. Cannon GA, Pashinski DJ, Lemon MR. 1991 Middepth flow near hydrothermal venting sites on the Southern Juan de Fuca Ridge. *J. Geophys. Res*. **96**, 12 815–12 831. (doi:10.1029/91JC01023)
52. Lee RW, Robert K, Matabos M, Bates AE, Juniper SK. 2015 Temporal and spatial variation in temperature experienced by macrofauna at Main Endeavour hydrothermal vent field. *Deep. Res. Part I Oceanogr. Res. Pap*. **106**, 154–166. (doi:10.1016/j.dsr.2015.10.004)
53. Johnson KS, Childress JJ, Beehler CL. 1988 Short-term temperature variability in the Rose Garden hydrothermal vent field: an unstable deep-sea environment. *Deep Sea Res. Part A. Oceanogr. Res. Pap*. **35**, 1711–1721. (doi:10.1016/0198-0149(88)90045-3)
54. Davenport J, Blackstock N, Davies DA, Yarrington M. 1987 Observations on the physiology and integumentary structure of the Antarctic pycnogonid *Decolopoda australis*. *J. Zool*. **211**, 451–465. (doi:10.1111/j.1469-7998.1987.tb01545.x)
55. Tjonneland A, Kland S, Nylund A. 1987 Evolutionary aspects of the arthropod heart. *Zool. Scr*. **16**, 167–175. (doi:10.1111/j.1463-6409.1987.tb00063.x)
56. Tjonneland A, Kryvi H, Ostnes JP, Okland S. 1985 The heart ultrastructure in two species of pycnogonids, and its phylogenetic implications. *Zool. Scr*. **14**, 215–219. (doi:10.1111/j.1463-6409.1985.tb00191.x)
57. Dresco-Derouet L. 1978 Métabolisme respiratoire de *Nymphon gracile* Leach et d'*Endeis spinosa* (Montagu) (Pycnogonida). *Cah. Biol. Mar*. **19**, 309–315.
58. Woods HA, Moran AL, Arango CP, Mullen L, Shields C. 2009 Oxygen hypothesis of polar gigantism not supported by performance of Antarctic pycnogonids in hypoxia. *Proc. R. Soc. B* **276**, 1069–1075. (doi:10.1098/rspb.2008.1489)
59. Bates AE, Lee RW, Tunnicliffe V, Lamare MD. 2010 Deep-sea hydrothermal vent animals seek cool fluids in a highly variable thermal environment. *Nat. Commun*. **1**, 1–14. (doi:10.1038/ncomms1014)
60. Cannon GA, Pashinski DJ. 1997 Variations in mean currents affecting hydrothermal plumes on the Juan de Fuca Ridge. *J. Geophys. Res*. **102**, 24 965–24 976. (doi:10.1029/97JC01910)
61. Pashinski DJ. 1998 The VENTS current observation program, 1984–1997 analysis: periodic motions, M2 and K1 tidal constituents, inertial and 4-day period forced motions. *US Dep. Commer. Natl. Ocean. Atmos. Adm. Environ. Res. Lab. Pacific Mar. Environ. Lab*.
62. Colaço A *et al.* 2006 Annual spawning of the hydrothermal vent mussel, *Bathymodiolus azoricus*, under controlled aquarium, conditions at atmospheric pressure. *J. Exp. Mar. Bio. Ecol*. **333**, 166–171. (doi:10.1016/j.jembe.2005.12.005)